

## An algebraic substructuring using multiple shifts for eigenvalue computations

Jin Hwan Ko<sup>1,\*</sup>, Sung Nam Jung<sup>1</sup>, Doyoung Byun<sup>1</sup> and Zhaojun Bai<sup>2</sup>

<sup>1</sup>Department of Aerospace Information Engineering, Konkuk University, Seoul, 143-701, South Korea

<sup>2</sup>Department of Computer Science, University of California at Davis, Davis, CA 95616, USA

(Manuscript Received May 17, 2007; Revised October 24, 2007; Accepted October 29, 2007)

---

### Abstract

Algebraic substructuring (AS) is a state-of-the-art method in eigenvalue computations, especially for large-sized problems, but originally it was designed to calculate only the smallest eigenvalues. Recently, an updated version of AS has been introduced to calculate the interior eigenvalues over a specified range by using a shift concept that is referred to as the *shifted AS*. In this work, we propose a combined method of both AS and the shifted AS by using multiple shifts for solving a considerable number of eigensolutions in a large-sized problem, which is an emerging computational issue of noise or vibration analysis in vehicle design. In addition, we investigated the accuracy of the shifted AS by presenting an error criterion. The proposed method has been applied to the FE model of an automobile body. The combined method yielded a higher efficiency without loss of accuracy in comparison to the original AS.

*Keywords:* Algebraic substructuring; Multiple shifts; Eigenvalue computation; Error criterion

---

### 1. Introduction

The dynamic analysis of vehicle structures often encounters a finite element discretization with many unknowns. The discretized models are typically used in many solutions, such as frequency response analysis at numerous frequencies. For large-sized systems, it is prohibited to compute the frequency responses directly because a factorization of the full size system matrices is required at each frequency. Hence, the mode superposition (MS) type method is a viable alternative to deal with this kind of large-sized problem. A large number of eigenvectors are needed as a basis of MS; then it becomes a major computational issue.

A famous approach for the partial eigensolution is a shift-invert Lanczos algorithm (SIL). When the number of the demanded eigenvalues is large, the necessity to choose additional shifts increases in order to

compensate for the slower convergence rate of the eigenvalue far from a shift [1]. Meanwhile, a full size matrix factorization is required at each shift, and this causes a dramatic increase in the computational cost for a large-sized problem. In addition, the selection of a series of shifts is a sophisticated process to improve the efficiency. Overall, the continual and compelling need for the frequency response analysis challenges the computational efficiency of the SIL.

Substructuring approaches, initially developed in early 1960s, have been revitalized in recent years, led by the automated multi-level substructuring (AMLS) method [2-4]. AMLS is a generalization of classical component mode synthesis techniques [5, 6] that has gained a good reputation for a commercially viable application. These approaches partition initial structures, namely system matrices, into a number of substructures, each of which is composed of substructures from the substructure of previous level, and so on. These substructures can be handled efficiently in single or multiple processor computing environments. A variation of the AMLS technique, referred to as the

---

\*Corresponding author. Tel.: +82 2 455 3842, Fax.: +82 2 444 6106  
E-mail address: jhko@aero.konkuk.ac.kr  
DOI 10.1007/s12206-007-1046-1

Algebraic substructuring (AS) method, has also been developed in [7, 8], and it is built upon the public codes of AS [7]. Meanwhile, the accuracy of these substructuring-based methods is known to be inferior to that of the Lanczos type method, and, typically, the accuracy worsens as the desired eigenvalue becomes farther from zero value.

Recently, an AS using a shift concept, which is referred to as the *shifted AS*, has been introduced to enhance the computational efficiency of modern microsystems operated over a high frequency range [9]. This new method is an extension of AS and has demonstrated the ability of obtaining the frequency response of a specified frequency range. It is shown that the higher accuracy for the frequency response is obtained by moving the location of a shift, thereby resolving the accuracy issue of the original AS.

In this work, we combine the shift AS and the original AS in order to calculate a large number of eigenvalues for a large-sized system. With a view of the technique that uses the multiple shifts for improvement of the efficiency of the Lanczos method [1], we adopt the multiple shifts concept to the combined AS method in a simple empirical way. A series of numerical experiments are executed to explore the accuracy of the shifted AS and the performance of the combined AS method using multiple shifts

The paper is organized as follows. In Section 2, we review the shifted AS and propose a criterion to predict the accuracy of the calculated eigenvalues. Section 3 presents the combined technique of AS and the shifted AS using multiple shifts. The numerical experiments on FE car body models are presented in Section 4 followed by concluding remarks.

## 2. Shifted algebraic substructuring

### 2.1 Review of basic theory

An updated version of AS that employs a shift concept has recently been introduced to solve problems in a range of eigenvalues  $[\lambda_l, \lambda_u]$  [9]. For simplicity, a single-level substructuring is presented in this section. A multi-level extension can be performed with the shifted matrices by using the same process which is described in [7].

Let us start from an  $N$ -size eigensystem with the shifted pencil  $(K^\sigma, M)$

$$K^\sigma q = \lambda^\sigma Mq, \tag{1}$$

where  $K^\sigma = K - \sigma M$  and  $\lambda^\sigma = \lambda - \sigma$ . The system matrices  $K$  and  $M$  are assumed to be constructed by FE discretizations. First, the rows and columns of  $K^\sigma$  and  $M$  are permuted so that these matrices are partitioned as

$$K^\sigma = \begin{matrix} & N_1 & N_2 & N_3 \\ \begin{matrix} N_1 \\ N_2 \\ N_3 \end{matrix} & \begin{bmatrix} K_{11}^\sigma & & \\ & K_{22}^\sigma & \\ & & K_{33}^\sigma \end{bmatrix} \end{matrix} \text{ and } M = \begin{matrix} & N_1 & N_2 & N_3 \\ \begin{matrix} N_1 \\ N_2 \\ N_3 \end{matrix} & \begin{bmatrix} M_{11} & & \\ & M_{22} & \\ & & M_{33} \end{bmatrix} \end{matrix}, \tag{2}$$

where the labels  $N_1$ ,  $N_2$ , and  $N_3$  indicate the dimensions of the sub-matrix blocks. This permutation is accomplished by applying a matrix ordering and partitioning algorithm such as the nested dissection algorithm to the structure of the matrix  $|K^\sigma| + |M|$ .  $(K_{11}^\sigma, M_{11})$  and  $(K_{22}^\sigma, M_{22})$  define two substructure blocks that are connected by a third block rows and columns of  $K^\sigma$  and  $M$ , which is the interface block.

Then, factorization is performed for the stiffness matrix of each block, resulting in the following decomposition form:

$$K^\sigma = L^T \widehat{K}^\sigma L, \tag{3}$$

where

$$L = \begin{bmatrix} I & & & \\ & (K_{11}^\sigma)^{-1} K_{13}^\sigma & & \\ & I & (K_{22}^\sigma)^{-1} K_{23}^\sigma & \\ & & & I \end{bmatrix}, \quad \widehat{K}^\sigma = \begin{bmatrix} K_{11}^\sigma & & \\ & K_{22}^\sigma & \\ & & \widehat{K}_{33}^\sigma \end{bmatrix}.$$

The last diagonal block of  $\widehat{K}^\sigma$  is given by

$$\widehat{K}_{33}^\sigma = K_{33}^\sigma - \sum_{i=1}^2 (K_{i3}^\sigma)^T (K_{ii}^\sigma)^{-1} K_{i3}^\sigma. \tag{4}$$

The congruent transformation of the pencil  $(K^\sigma, M)$  by  $L$  yields the eigensystem of a new pencil  $(\widehat{K}^\sigma, \widehat{M})$ :

$$\widehat{K}^\sigma \widehat{q} = \lambda^\sigma \widehat{M} \widehat{q}, \tag{5}$$

where  $\widehat{K}^\sigma$  is defined in Eq. (3),

$$\widehat{M} = L^{-T} M L^{-1} = \begin{bmatrix} M_{11} & & \widehat{M}_{13} \\ & M_{22} & \widehat{M}_{23} \\ \widehat{M}_{31} & \widehat{M}_{32} & \widehat{M}_{33} \end{bmatrix},$$

and

$$\begin{aligned} \widehat{M}_{i3} &= M_{i3} - M_{ii}(K_{ii}^\sigma)^{-1}K_{i3}^\sigma, \\ \widehat{M}_{33} &= M_{33} - \sum_{i=1}^2 \{(K_{i3}^\sigma)^T(K_{ii}^\sigma)^{-1}M_{i3} \\ &\quad + M_{i3}^T(K_{ii}^\sigma)^{-1}K_{i3}^\sigma - (K_{i3}^\sigma)^T(K_{ii}^\sigma)^{-1}M_{ii}(K_{ii}^\sigma)^{-1}K_{i3}^\sigma\} \end{aligned}$$

The pencil  $(\widehat{K}^\sigma, \widehat{M})$  is known as the Craig-Bampton (C-B) form [6] in structural engineering. The eigenvalues of  $(\widehat{K}^\sigma, \widehat{M})$  are identical to those of  $(K^\sigma, M)$ , and the properties of the system matrices after the transformation are preserved. Note that an eigenvector is calculated by  $q = L^{-1}\hat{q}$ , where  $\hat{q}$  is an eigenvector of  $(\widehat{K}^\sigma, \widehat{M})$ .

The next step of AS is to extract the eigenvectors/eigenvalues of each substructure and interface, i.e., eigenpairs of the pencils  $(\widehat{K}_{ii}^\sigma, \widehat{M}_{ii})$ . These eigenvectors are referred to as the *subeigenvectors*, and the corresponding eigenvalues are referred to as the *subeigenvalues*. The range of the subeigenvalues is given by  $[\mu_1^\sigma, \mu_n^\sigma]$ , whose ends are called the *cutoff values*. Let the projection matrix be defined as

$$S = \begin{matrix} & m_1 & m_2 & m_3 \\ \begin{matrix} N_1 \\ N_2 \\ N_3 \end{matrix} & \begin{bmatrix} S_1 & & \\ & S_2 & \\ & & S_3 \end{bmatrix} \end{matrix}, \quad (6)$$

where  $S_1$ ,  $S_2$  and  $S_3$  consist of  $m_1$ ,  $m_2$ , and  $m_3$  retained subeigenvectors in each block. Meanwhile, most of the subeigenvectors are truncated, then  $m = m_1 + m_2 + m_3$  is much less than  $N$ . The subspace  $\Psi$  is spanned by column vectors of  $S$ , that is,  $\Psi = \text{span}\{S\}$ .

By orthogonally projecting the pencil  $(\widehat{K}^\sigma, \widehat{M})$  onto the subspace  $\Psi$ , we then have the eigensystem

$$K_m^\sigma \phi = \theta^\sigma M_m \phi, \quad (7)$$

where  $K_m^\sigma$  and  $M_m$  are  $m \times m$  matrices defined as  $K_m^\sigma = S^T \widehat{K}^\sigma S$  and  $M_m = S^T \widehat{M} S$ . This follows the form of the standard Rayleigh-Ritz theory that  $\theta^\sigma$  is the best approximation of the eigenvalues  $\lambda^\sigma$  and the vector formed by  $q = L^{-1}S\phi$  provides an approximation to the corresponding eigenvector of Eq. (1) [10].

In particular, when the shift is set by  $\sigma = 0$ , there are no low truncated subeigenvectors. Subsequently, the procedures in this section become the same as the original AS.

### 2.2. Accuracy

The impact of retained subeigenvectors on the accuracy of eigenvalues has been an important issue in the study of the AMLS and AS algorithms [3], [8]. Here, we explore the effectual factors on the accuracy of the shifted AS by using the retained subeigenvectors. As noted earlier,  $(\widehat{K}^\sigma, \widehat{M})$  and  $(K^\sigma, M)$  have the same set of eigenvalues. If  $\hat{q}$  is an eigenvector of  $(\widehat{K}^\sigma, \widehat{M})$ , then  $q = L^{-1}\hat{q}$ .

Let  $((\mu^\sigma)_j^i, v_j^i)$  be the  $j$ -th eigenpair of the  $i$ -th subproblem ( $i=1,2$ ) and  $((\mu^\sigma)_3^i, v_3^i)$  be the eigenpair of the interfacial problem:

$$\begin{aligned} K_{ii}^\sigma v_j^i &= (\mu^\sigma)_j^i M_{ii} v_j^i \quad \text{for } i=1,2 \\ \widehat{K}_{33}^\sigma v_3^i &= (\mu^\sigma)_3^i \widehat{M}_{33} v_3^i \end{aligned} \quad (8)$$

Let the truncated subeigenvalues by the low cutoff value  $\mu_l$  be ordered as

$$(\mu^\sigma)_1^i < (\mu^\sigma)_2^i < \dots < (\mu^\sigma)_{nl}^i \quad (9)$$

and the truncated subeigenvalues by the upper cutoff value  $\mu_u$  be ordered as

$$(\mu^\sigma)_{N_i-nu+1}^i < (\mu^\sigma)_{N_i-nu+2}^i < \dots < (\mu^\sigma)_{N_i}^i, \quad (10)$$

where  $nl$  is the number of the low truncated subeigenvalues and  $nu$  is the number of the upper truncated subeigenvalues of the  $i$ -th block.

To analyze the effect of the truncated subeigenvectors to the eigenvalue, we first express  $\hat{q}$  of Eq. (5) as

$$\hat{q} = \begin{bmatrix} V_1 & & \\ & V_2 & \\ & & V_3 \end{bmatrix} \begin{bmatrix} y_1 \\ y_2 \\ y_3 \end{bmatrix}, \quad (11)$$

where  $V_i = \{v_1^i, \dots, v_{N_i}^i\}$ ,  $i=1,2,3$ , and  $y = \{y_1^T, y_2^T, y_3^T\}^T \neq 0$ . After pre-multiplying  $V^T$ , the generalized eigenvalue problem of (5) yields

$$\begin{bmatrix} N_1^\sigma & & \\ & N_2^\sigma & \\ & & N_3^\sigma \end{bmatrix} \begin{bmatrix} y_1 \\ y_2 \\ y_3 \end{bmatrix} = \lambda^\sigma \begin{bmatrix} I_1 & & G_{13} \\ & I_2 & G_{23} \\ G_{13}^T & G_{23}^T & I_3 \end{bmatrix} \begin{bmatrix} y_1 \\ y_2 \\ y_3 \end{bmatrix}, \quad (12)$$

where

$$\begin{aligned} N_i^\sigma &= \text{diag}((\mu^\sigma)_1^i, (\mu^\sigma)_2^i, \dots, (\mu^\sigma)_{N_i}^i) \quad \text{for } i=1,2,3 \\ G_{i3} &= V_i^T \widehat{M}_{i3} V_3 \quad \text{for } i=1,2. \end{aligned}$$

Suppose  $N_i^\sigma - \lambda^\sigma I_i$  is nonsingular for  $i=1,2,3$ . It follows from each block of (12) that

$$\begin{aligned} y_i &= (N_i^\sigma - \lambda^\sigma I_i)^{-1} \lambda^\sigma G_{i3} y_3 \quad \text{for } i=1,2 \\ y_3 &= (N_3^\sigma - \lambda^\sigma I_3)^{-1} \lambda^\sigma (G_{13}^T y_1 + G_{23}^T y_2) \end{aligned} \quad (13)$$

Consequently, we can express the  $j$ -th element of  $y_i$  by

$$|e_j^T y_i| = \rho_{\lambda^\sigma}((\mu^\sigma)_j^i) g_j^i, \quad (14)$$

where

$$\begin{aligned} \rho_{\lambda^\sigma}((\mu^\sigma)_j^i) &= \left| \lambda^\sigma / ((\mu^\sigma)_j^i - \lambda^\sigma) \right|, \\ g_j^i &= |e_j^T G_{i3} y_3| \quad \text{for } i=1,2 \text{ and } g_j^3 = |e_j^T (G_{13}^T y_1 + G_{23}^T y_2)|. \end{aligned}$$

When  $|g_j^i| \in [\gamma_1, \gamma_2]$  for some modest-size constants  $\gamma_1 < \gamma_2$ , the magnitude of  $|e_j^T y_i|$  is essentially determined by  $\rho_{\lambda^\sigma}((\mu^\sigma)_j^i)$ , which means the contribution of  $j$ -th subeigenvector to the solution  $y$  [7]. The form of  $\rho_{\lambda^\sigma}((\mu^\sigma)_j^i)$  is first introduced by [8] and is called  $\rho$ -factor. It is easy to see that  $\rho_{\lambda^\sigma}((\mu^\sigma)_j^i)$  is large when  $(\mu^\sigma)_j^i$  is close to  $\lambda^\sigma$ , and it becomes small when  $(\mu^\sigma)_j^i$  is away from  $\lambda^\sigma$ . Hence, the subeigenvectors, whose corresponding subeigenvalues are close to  $[\lambda_l^\sigma, \lambda_u^\sigma]$ , should be retained. Namely, the condition  $[\lambda_l^\sigma, \lambda_u^\sigma] \subset [\mu_l^\sigma, \mu_u^\sigma]$  is necessary. Therefore, it is trivial to show that  $\rho_{\lambda^\sigma}((\mu^\sigma)_j^i)$  is monotonically increasing in the left part of the low cutoff value and decreasing in the right part of the upper cutoff value as follows:

$$\begin{aligned} \rho_{\lambda^\sigma}((\mu^\sigma)_1^i) &< \rho_{\lambda^\sigma}((\mu^\sigma)_2^i) < \dots < \rho_{\lambda^\sigma}((\mu^\sigma)_{n_l}^i) \\ \text{because } \mu_l^\sigma &< \lambda_l^\sigma \end{aligned} \quad (15)$$

and

$$\begin{aligned} \rho_{\lambda^\sigma}((\mu^\sigma)_{N_l - m_u + 1}^i) &> \rho_{\lambda^\sigma}((\mu^\sigma)_{N_l - m_u + 2}^i) > \dots > \rho_{\lambda^\sigma}((\mu^\sigma)_{N_l}^i) \\ \text{because } \mu_u^\sigma &> \lambda_u^\sigma. \end{aligned} \quad (16)$$

If the relative distance between the subeigenvalue and the eigenvalue,  $\mu^\sigma - \lambda^\sigma$ , is fixed, the  $\rho$ -factor decreases as  $\lambda^\sigma$  becomes smaller. In order to minimize magnitude of the shifted eigenvalues, the shift should be located in the center of the range by

$$\sigma = \frac{\lambda_l + \lambda_u}{2}, \quad (17)$$

then

$$\lambda_l^\sigma = -\lambda_u^\sigma. \quad (18)$$

By using this location, the eigenvalue range is divided into two half ranges, namely, left half and right

half. For the eigenvalues in the right half, the monotonic decrease in (16) as the subeigenvalues is further from the shift is the same aspect as the original AS method. Meanwhile, the eigenvalues in the left half are negative. Hence, we reordered (9) in terms of an absolute value, which means the distance from the shift, as

$$|\lambda_l^\sigma| < |(\mu^\sigma)_{n_l}^i| < \dots < |(\mu^\sigma)_2^i| < |(\mu^\sigma)_1^i|. \quad (19)$$

Then the  $\rho$ -factors of (15) can be rewritten as

$$\rho_{\lambda^\sigma}((\mu^\sigma)_{n_l}^i) > \dots > \rho_{\lambda^\sigma}((\mu^\sigma)_2^i) > \rho_{\lambda^\sigma}((\mu^\sigma)_1^i). \quad (20)$$

Consequently, in view of the distance from the shift, the  $\rho$ -factors in the left half also decrease monotonically the further the subeigenvalues are from the shift. In addition, the truncated subeigenvectors in left part can also affect the accuracy of eigenvalues in the right half and vice versa. In those cases, the aspect of the monotonic decrease is preserved as well.

Based on the monotonic decrease in the both ranges, the cutoff values are determined by simply multiplying a coefficient to the end of the range, a similar method to the previous works, as

$$\mu_l^\sigma = c_l \lambda_l^\sigma, \quad \mu_u^\sigma = c_u \lambda_u^\sigma, \quad (21)$$

where  $c_u > 1$  and  $c_l > 1$  are referred to as the *relaxation factors*. As the large  $c_l, c_u$  are used, the accuracy is expected to be better. On the other hand, it makes the number of the retained subeigenvectors increase and results in an increase in computational cost.

The  $\rho$ -factor of the truncated subeigenvector in the left part has the largest value when the desired eigenvalue is close to  $\lambda_l^\sigma$ , and the  $\rho$ -factor in the right part becomes largest when the desired eigenvalue is near  $\lambda_u^\sigma$ . The maximum  $\rho$ -factors are

$$\begin{aligned} \rho_{\max}(|(\mu^\sigma)_i| > |(\mu^\sigma)_1|) &= \rho_{\lambda_l^\sigma} = \left| \frac{\lambda_l^\sigma}{c_l \lambda_l^\sigma - \lambda_l^\sigma} \right| = 1/c_l - 1, \\ \rho_{\max}((\mu^\sigma)_i > (\mu^\sigma)_u) &= \rho_{\lambda_u^\sigma} = \left| \frac{\lambda_u^\sigma}{c_u \lambda_u^\sigma - \lambda_u^\sigma} \right| = 1/c_u - 1. \end{aligned} \quad (22)$$

Next, we make the two relaxation factors equal in order that the maximum  $\rho$ -factors in the both parts become the same. This is a way to balance the errors of both parts by

$$c_l = c_u. \quad (23)$$

The effect of the relaxation factors looks the same as the original AS; however, the major advantage of

the shifted AS is due to the magnitude of the shifted eigenvalue. One can easily recognize that the shifted eigenvalue  $\lambda^\sigma$  is much smaller than the original eigenvalue  $\lambda$ ; subsequently, the shifted AS requires a smaller range of subeigenvalues than the original AS. The fact greatly reduces the computational cost when the subeigenvectors whose  $\rho$ -factors have the same level of magnitude are truncated by the same  $c_u$  value.

Here, the accuracy is estimated considering the mode selection strategy, which is based merely on a  $\rho$ -factor threshold except the magnitude of  $g_j^i$ . Many researchers are currently investigating a number of ways to estimate the magnitude of  $g_j^i$ . Future research on this topic can provide a more precise error bound.

In particular, when no shift exists, that is,  $\sigma = 0$  and  $nl = 0$ , the  $\rho$ -factor becomes

$$\rho_\lambda(\mu_j^i) = |\lambda(\mu_j^i - \lambda)| = |\lambda(c_u \lambda_u - \lambda)|. \quad (24)$$

Then, the  $\rho$ -factor has the largest values at the upper cutoff value  $\lambda_u$  as

$$\rho_{\max}(\mu_i > \mu_u) = \rho_{\lambda_u} = 1/c_u - 1. \quad (25)$$

As described in this section, the error of the computed Ritz values decreases by increasing the relaxation factors. Now we consider another expression about the accuracy of the Ritz value and also corresponding Ritz vector in the particular case. When the first Ritz value  $\theta_1$  close to  $\lambda_1$  is computed, the errors between the Ritz pair and the eigenpair are bounded as follows:

$$\theta_1 - \lambda_1 \leq (\lambda_N - \lambda_1) \sin^2 \angle_M(q_1, \mathfrak{N}), \quad (26-1)$$

$$\sin \angle_M(X\phi_1, q_1) \leq \sqrt{\frac{\lambda_N - \lambda_1}{\lambda_2 - \lambda_1}} \sin \angle_M(q_1, \mathfrak{N}), \quad (26-2)$$

where  $\angle_M(X\phi_1, q_1)$  denotes the  $M$ -angle between the two vectors,  $X$  is  $L^{-1}S$  and  $\mathfrak{N}$  is the subspace that is spanned by the column vectors of  $X$ . These are from Theorem 3.1 of [8]. According to (26-1),  $\sin \angle_M(q_1, \mathfrak{N})$ , which is typically defined by a positive value, is expected to decrease when the accuracy improves by retaining a larger number of the subeigenvectors; subsequently, the  $M$ -angle between the Ritz vector and the eigenvector in (26-2) can be reduced. It still remains as a challenging problem to find the error bounds of interior eigenpairs in the general case.

### 3. AS using multiple shifts

The demand of a large number of eigenpairs is increasing more in a vehicle's noise or vibration analysis than in past years. According to the recent research by Kropp et al. [11], over 5,000 eigenvectors are required for a vibro-acoustic analysis up to 800 Hz. When numerous eigenpairs are required, a Lanczos type method faces difficulties in terms of the computational cost and memory usage because it deals with a full-sized system. Meanwhile, an AS type method efficiently calculates approximate eigenpairs by solving the projected eigenproblem on the smaller subspace, which is composed of retained subeigenvectors. However, the AS method has been developed to calculate only the smallest eigenvalues, and the accuracy of an eigenvalue is worse as the distance from zero increases. Recently, an updated version of AS was introduced as the shifted AS, which solves interior eigenvalues and improves accuracy of the solved eigenvalues by moving a shift [9]. Here, we combine the original AS and the shifted AS and adopt the multiple shifts idea to solve a considerably large number of eigenpairs.

According to Section 2.1, AS or the shifted AS is separated into four main steps. Step 1 is the partition and rearrangement of the system matrices ((1)-(2)); step 2 is C-B transform ((3)-(6)); step 3 is solving each subproblem to construct (7), and step 4 is solving the projected eigenproblem (8). When the demanded number of the eigenvalues increases, the computational cost of steps 3-4, which are relative to solving the eigenpairs, can be more expensive than that of step 2.

When a Lanczos type method calculates numerous eigenpairs, the techniques using multiple shifts in a heuristic way reduce the computational cost. Inspired by this, we divide the whole range into several subranges, which includes one shift in order to reduce the computational burden of the eigensolution. However, the Craig-Bampton transform is repeated for each shift as a counter factor, just as one factorization of each shift is required in the Lanczos type method. After the division, the original AS is applied to the first subrange because it already performs excellently when calculating the smallest eigenvalues. Then, the shifted AS is applied to other subranges. This combined method using multiple shifts is referred to as ASEIG<sup>MS</sup>. As can be observed, the computations of the eigenvalues in each subrange are absolutely inde-

pendent of each other; hence, ASEIG<sup>MS</sup> can be easily extended to a parallel version.

Note that ASEIG<sup>MS</sup> requires a number of parameters. Some of them are regulated, such as the location of a shift by (17) and the relationship between  $c_l, c_u$  by (23). Here we count on the relaxation factors and the number of the subranges (shifts). Both of them are not regulated; hence, we choose the proper values through our numerical experience.

First, the relaxation factor plays an important role in determining the range of the subeigenvalues to be retained and has a strong effect on the accuracy of the computed eigenvalues. Hence, how to determine the value depends on the desired level of accuracy. As the relaxation factor increases, more subeigenvectors are retained, resulting in the improvement of the accuracy, which is mathematically verified in [3] the best of our knowledge, the strict criterion of the relaxation factor which affects the accuracy has not been introduced so far; hence, most researchers use an empirical method to increase the factor by a certain increment until the desired accuracy is satisfied. In Kaplan's thesis, relaxation factors between 9 and 100 are utilized to explore the influence of the accuracy, and there is an order of magnitude reduction in the error when changing from 9 to 56.2 (see Fig. 7.16 in [4]). For the shifted AS, the accuracy is also expected to improve by increasing the relaxation factors because our proposed criterion in Section 2.2 was developed based on previous research.

Second, the method to divide the subranges is a major factor of the efficiency of ASEIG<sup>MS</sup> for computing a considerably large number of eigenvalues. To balance the computational cost of each range, ASEIG<sup>MS</sup> needs to make the number of eigenvectors in each subrange similar because the cost is mainly dependent upon it. However, the shifted AS cannot easily automatically assign a similar number to each subrange, so we simply divide the original range by the same spacing.

ASEIG<sup>MS</sup> has been developed on top of ASEIG code [7]. In the code, the multilevel partition is done by MeTiS [12]. The eigenvalues and the subeigenvalues of the substructure blocks are computed by ARPACK [13] with SuperLU [14], and the subeigenvalues in the interfacial block are solved by LAPACK [15]. The level of substructuring is determined automatically by the default parameter values of MeTiS, and the tolerance of SIL subroutine in ARPACK is set by  $10^{-10}$ .

As we discussed in section 2.2, the accuracy of the computed eigenvalues by AS-type methods improves and their range within a desired accuracy becomes wider as the relaxation factors are larger; thus, a smaller number of subranges are required through the whole range. In this case, the cost of the C-B transformation, which is demanded for each shift, is reduced, but there should be more cost for computing the projected eigenpairs, which means Ritz pairs. When smaller relaxation factors are used, the number of subranges should be larger to satisfy the desired accuracy. In that case, we face the opposite situation. Hence, a parameter tuning procedure of the relaxation factor and the number of the subranges depends on the experience of the cost growth in the C-B transformation and the eigensolution. The cost of the transformation relies on the performance of a factorization code such as SuperLU and a linear algebra code. The cost of the eigensolution depends on the performance of an eigensolver such as ARPACK.

We will compare the performance of ASEIG<sup>MS</sup> with the original AS and shift-invert Lanczos in the next section. Let us briefly review these methods.

Shift and invert Lanczos using multiple shifts: The public code ARPACK contains an SIL subroutine for the eigenproblem and is used for calculating the eigenpairs of the pencil  $(K, M)$ . It employs the same tolerance of  $10^{-10}$ .

ASEIG: The original AS method in which the shift is zero and the substructuring level is given based on the size of the original problem. The relaxation factor  $c_u$  is determined depending on the desired accuracy.

ASEIG<sup>MS</sup>: The shift is determined by Eq. (17) and  $c_l, c_u$  are given by same values based on the (23). The number of subranges and the value of relaxations factors are determined based on the efficiency and accuracy issue in an empirical way.

#### 4. Numerical experiments and discussion

Proper management of a vehicle's noise or vibration characteristics helps to produce a more competitive product. The mode superposition (MS) is a viable alternative in a numerical analysis where a larger number of eigenvectors are required as a basis. The wider the required range of interest, the larger the number of eigenpairs that should be utilized. Subsequently, finding an efficient solution scheme is one of the major computational issues in vehicle design.

We are starting from a geometric model of the

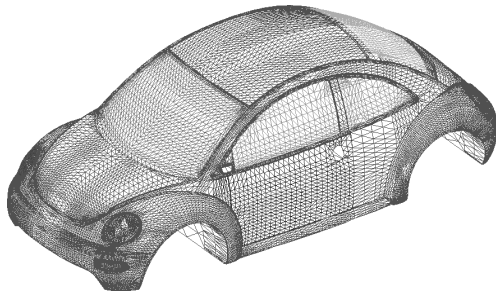


Fig. 1. Fine fe model of the car body of a new beetle.

Volkswagen New Beetle. The model is discretized by FE shell elements. All experiments were conducted on a platform that has a 1.6 GHz Itanium II processor. This computer has 15 gigabytes (GB) of physical memory and 100 GB of disk space. The operating system is Red Hat Linux 3.2.3-42. Two different kinds of FE model are employed to exploit the salient features of the proposed methodology. The degrees of freedom are 38 k (coarse) and 152 k (fine), respectively. Fig. 1 shows the FE model having 152 k unknowns.

#### 4.1. Parametric study

The coarse FE model is utilized to investigate the accuracy and the efficiency of the solution schemes. The range of eigenvalues considered in the parametric study is  $[0, 8e6]$ , and the range of frequencies falls around  $[1, 450]$  Hz. The substructuring level is automatically determined to be 8 in the MeTiS library. In this situation, 256 substructures and 236 interface blocks are automatically generated.

##### 4.1.1 The effect of the relaxation factor on the accuracy

Among the whole range, a given interior range  $[7e6, 8e6]$  is selected to investigate the accuracy by changing the relaxation factor of the shifted AS. The relaxation factor is increased by 5, 25, and 50. The error percentage is measured with respect to the eigenvalues obtained from SIL, and the results are presented in Fig. 2. Percent error in the figure is computed by

$$\left| \frac{\lambda_{SIL} - \lambda}{\lambda_{SIL}} \right| \times 100 \text{ (\%)}$$

The computational time grows by 127, 206, 282 seconds as the relaxation factors are varied from  $c_l = c_u = 5, 25, 50$ , respectively.

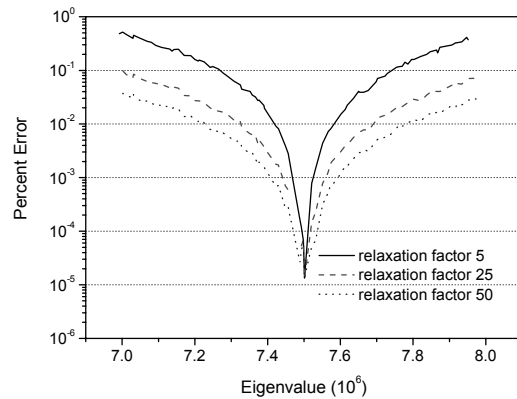


Fig. 2. Effect of the relaxation factor on the accuracy of eigenvalues for the coarse model.

Table 1. AS data, elapsed time, and accuracy of ASEIG for the coarse model.

AS data		Elapsed time (sec.)					Accuracy
# eigenvalues	# subeigenvalues	Step 1	Step 2	Step 3	Step 4	Total	Max. error (%)
945	6,609	1	64	7	2,775	2,847	1.0

The accuracy of the shifted AS improves by increasing the relaxation factor, as is expected. There is an order of magnitude reduction in the error when the relaxation factors are changed from 5 to 50. In Fig. 2, we can also observe that a highly accurate prediction of the eigenvalues near the shift is obtained compared with those far from the shift.

##### 4.1.2 The number of shifts (subranges) on the efficiency

In Table 1, AS data, elapsed time, and accuracy are presented when the ASEIG is applied to the whole range  $[0, 8e6]$ . The relaxation factor is set at 15 to obtain around 1% relative error.

As the table indicates, the elapsed time of step 4 is 43 times that of step 2. Step 1 and step 3 require relatively small computational cost. The computational cost of step 4 can be reduced by dividing it into several subranges because the number of eigenvalues for each subrange becomes smaller than 945. On the other hand, dividing the problem causes an increase in the cost of step 2 and step 3 because the C-B transform of step 2 is repeated by the number of shifts and the subproblems of step 3 must also be solved for each shift.

Based on the smaller than 1% error in Fig. 2 when the relaxation factor is given by  $c_l = c_u = 5$ , we em-

Table 2. Elapsed time and accuracy of ASEIG<sup>MS</sup> with the same relaxation factor when varying the number of subranges for the coarse model.

Width (106)	# subranges	Elapsed time (sec.)					Accuracy	
		Step 1	Step 2	Step 3	Step 4	Total	Max. error (%)	
2	4	3	225	20	879	1,127	7.2	
1	8	3	446	40	516	1,005	7.6	
0.5	16	3	888	78	379	1,348	7.5	

ploy the same relaxation factor in each subrange. We first divide the whole range in the same spacing by 2e6, 1e6, 0.5e6 and compare the performance of each case. The original AS is applied to the first subrange because it does not have truncated subeigenvectors in the left part. Other subranges are solved by the shifted AS. Table shows their performance with a given eigenvalue width.

As the number of subranges increases, the elapsed times of steps 2 increase by the same ratio as the number of subranges does, but that of step 4 decreases since the size of the projected system is smaller in each subrange. The costs of step 1 and step 3 are relatively small portions of the total cost. With the same relaxation factor, the error percentages are similar in the different widths and the elapsed time in the case of 1e6 is smaller, so 1e6 is the best choice. However, the accuracy is poor because the error of each subrange is not a similar level. Therefore, ASEIG<sup>MS</sup> needs different relaxation factors for the subranges with a certain rule.

**4.1.3 Subrange vs. relaxation factors**

As an adjustment method for each subrange, we reduced the relaxation factor by a certain amount as the subrange goes higher. For instance, the first subrange uses 19, and then it is reduced by an increment 2. Then the relaxation factor of the last subrange becomes 5. The results of the accuracy are compared to ASEIG<sup>MS</sup> with the same relaxation factors in Fig. 3.

When those relaxation factors are employed, the total elapsed time increases slightly to 1,257 seconds, but the accuracy becomes better. Consequently, the total computational cost of ASEIG with 1.0% maximum error is 2,847 seconds, and ASEIG<sup>MS</sup> with 1.3% maximum error takes less computational time, 1,257 seconds. Each subrange can be independently processed, so the ASEIG<sup>MS</sup> is expected to improve the performance when a parallel version of it is developed.

Table 3. AS data, elapsed time, and accuracy of ASEIG for the fine model.

AS data		Elapsed time (sec.)					Accuracy	
# eigenvalues	# subeigenvalues	Step 1	Step 2	Step 3	Step 4	Total	Max. error (%)	
1,605	15,374	8	665	50	18,074	18,797	1.5	

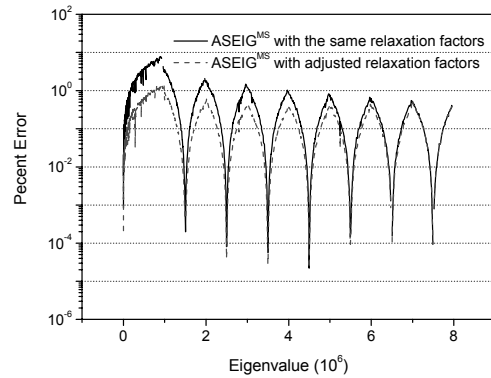


Fig. 3. Percent of error when adjusting the relaxation factor of each subrange of ASEIG<sup>MS</sup> for the coarse model.

**4.2 Performance of a wide range**

When an FE model is used for dynamic analysis in a wide range, a larger model with more eigenpairs is required. Hence, we employ a fine model for the wider range [0, 1.6e7], and the range of the frequencies falls around [1, 636] Hz. The substructuring level is automatically determined to be 10 in the MeTiS library. In this situation, 1,024 substructures and 927 interfaces are automatically generated. The relaxation factor for ASEIG is determined by  $c_u = 15$  to obtain around 1% error. First, we tabulate the AS data, elapsed time, and accuracy in Table 3 when ASEIG is applied to the fine model.

According to the results in Table 3, the computational cost of step 4 is 27 times that of step 2. As the size of the problem becomes larger, the cost of the C-B transform sharply increases. However, step 4 is expected to somewhat slow the increase of the computational cost because the number of subeigenvalues in the same range is not seriously varied; hence, the ratio of step 4 to step 2 in terms of the elapsed time of the fine model is smaller than that of the coarse model. The elapsed times of steps 1 and 3 are relatively small, which is a similar phenomenon to that of the coarse model. Subsequently, the whole range should be divided to reduce the computational cost of step 4. Here, we divide the range into eight subranges, and the relaxation factors of the subranges are determined to

Table 4. Elapsed time and accuracy of ASEIG<sup>MS</sup> with the adjusted relaxation factors for the fine model.

Width (106)	# subranges	Elapsed time (sec.)					Accuracy
		Step 1	Step 2	Step 3	Step 4	Total	Max. error (%)
2	8	13	4,567	370	5,462	10,412	1.6

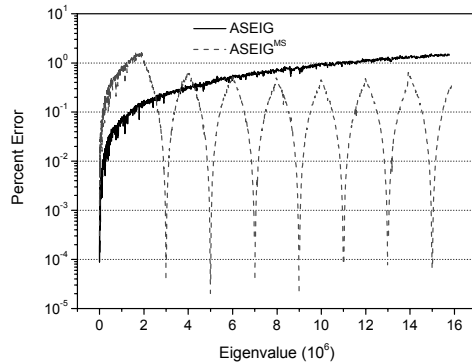


Fig. 4. Percent of error of ASEIG and ASEIG<sup>MS</sup> with the adjusted relaxation factors for the fine model.

be same values by the adjusted method mentioned in Section 4.1. The elapsed time and the accuracy for the fine model are listed in Table 4, and the percent errors of ASEIG<sup>MS</sup> are depicted in comparison to the ASEIG over the whole range in Fig. 4.

It is indicated from the results of Table 4 that the elapsed times of steps 2 and 4 have a similar order of magnitude, while those of steps 1 and 3 are relatively small. Considering Table 3 and Table 4, the total computation time has been dramatically reduced from 18,797 to 10,412 seconds. Also, the maximum error of ASEIG<sup>MS</sup> is about 1.6 %, which is similar to the case of ASEIG, as can be seen in Table 3. Consequently, the ASEIG<sup>MS</sup> improves the efficiency of ASEIG for the large-sized model of the wide eigenvalue range with a similar level of the accuracy. It is indicated in Fig. 4 that ASEIG<sup>MS</sup> dramatically improves the accuracy at each shift over the whole range of eigenvalues and leads to a lower error percentage compared with ASEIG, even though they possess similar numbers of maximum errors.

In addition, SIL type methods are known to be more costly than AS type methods since the former deal with full-sized systems while providing a relative high level of accuracy of the calculated eigenvalues [3], [7]. For the fine model, the computation time of the SIL with no shift takes 88,719 seconds, while the ASEIG<sup>MS</sup> takes 67,410 seconds.

## 5. Concluding remarks

In this work, a combined method of AS and a shifted AS using multiple shifts is proposed to calculate a considerable number of eigenvalues for a large-sized problem, which is an emerging computational issue of a noise or vibration analysis in vehicle design. We first proposed  $\rho$ -factor of the shifted AS to measure the accuracy of the solution from the perspective of the retained subeigenvectors. The relaxation factors were utilized to obtain the desired accuracy of the eigenvalues, and the number of shifts was determined by balancing the computational cost of the C-B transform and that of the eigensolution of the projected eigensystem. The numerical experiments on the FE model of a car body demonstrated that the combined method results in improved efficiency without loss of accuracy in comparison to the original AS. Future research should involve a frequency response analysis over a wide range of a vibro-acoustic analysis, parallelization, and an automatic parameter decision.

## Acknowledgments

This study is supported by the Korea Research Foundation Grant funded by the Korean Government (MOEHRD) (KRF-2006-005-J03301) and BK 21 Education Program of ST-IT Fusion.

## References

- [1] G. R. Grimes, J. G. Lewis and H. D. Simon, A shifted block Lanczos algorithm for solving sparse symmetric generalized eigenproblems, *SIAM J. Matrix Anal. Appl.* 15 (1) (1994).
- [2] J. K. Bennighof and C. K. Kim, An adaptive multi-level substructuring method for efficient modeling of complex structures, Proceedings of the AIAA 33rd SDM Conference, Dallas, Texas, (1992) pp. 1631-1639.
- [3] J. K. Bennighof and R. B. Lehoucq, An Automated Multilevel Substructuring Method for Eigenspace Computation in Linear ElastoDynamics, *SIAM Journal on Scientific Computing* 25 (6) (2004) 2084-2106.
- [4] M. F. Kaplan, Implementation of automated multi-level substructuring for frequency response analysis of structures, PhD thesis, University of Texas at Austin, (2001).

- [5] W. C. Hurty, Vibration of structural systems by component mode synthesis, *J. Engrg. Mech. Division, ASCE*, 86 (1960) 51-69.
- [6] R. R. Craig Jr. and M.C.C. Bampton, Coupling of substructures for dynamic analysis, *AIAA Journal* 6 (7) (1968) 1313-1319.
- [7] W. Gao, X.S. Li, C. Yang and Z. Bai, An implementation and evaluation of the AMLS method for sparse eigenvalue problems, Technical Report LBNL-57438, Lawrence Berkeley National Laboratory, (2006).
- [8] C. Yang, W. Gao, Z. Bai, X. Li, L. Lee, P. Husbands and E. Ng, An algebraic substructuring method for large-scale eigenvalue calculations, *SIAM J. Sci. Comput.* 27 (3) (2005) 873-892.
- [9] J. H. Ko and Z. Bai, An Algebraic Substructuring Method for High-Frequency Response Analysis of Micro-systems, International conference of computational science 2007, *LNCS 4487*, (2007) 521-528.
- [10] B. N. Parlett, the symmetric eigenvalues problems, Prentice-Hall, (1980).
- [11] A. Kropp and D. Heiserer, Efficient Broadband Vibro-Acoustic Analysis of Passenger Car Bodies Using an FE-based Component Mode Synthesis Approach, Fifth World Congress on Computational Mechanics, Vienna, Austria (2002).
- [12] G. Karypis, MeTiS, Department of Computer Science and Engineering at the University of Minnesota, <http://www-users.cs.umn.edu/~karypis/metis/metis/index.html>, (2006).
- [13] R. Lehoucq, D. C. Sorensen and C. Yang, ARPACK User's Guide: Solution of Large-Scale Eigenvalue Problems with Implicitly Restarted Arnoldi Methods, SIAM, Philadelphia, (1998).
- [14] J. W. Demmel, S. C. Eisenstat, J. R. Gilbert, X. S. Li and J. W. H. Liu, A supernodal approach to sparse partial pivoting, *SIAM J. Matrix Anal. Appl.* 20 (3) (1999) 720-755.
- [15] E. Anderson, Z. Bai, C. Bischof, S. Blackford, J. Demmel, J. Dongarra, J. Du Croz, A. Greenbaum, S. Hammarling, A. McKenney and D. Sorensen, LAPACK Users' Guide 3-rd, SIAM, (1999).